



**HAL**  
open science

## Seasonal dynamics of transparent exopolymer particles (TEP) and their drivers in the coastal NW Mediterranean Sea

Eva Ortega-Retuerta, Eva Ortega-Retuerta, Cèlia Marrasé, Ana Muñoz-Fernández, M Montserrat Sala, Rafel Simó, Josep M Gasol, Eva Ortega-Retuerta, Cèlia Marrasé, Ana Muñoz-Fernández, et al.

### ► To cite this version:

Eva Ortega-Retuerta, Eva Ortega-Retuerta, Cèlia Marrasé, Ana Muñoz-Fernández, M Montserrat Sala, et al.. Seasonal dynamics of transparent exopolymer particles (TEP) and their drivers in the coastal NW Mediterranean Sea. *Science of the Total Environment*, 2018, 631-632, pp.180-190. 10.1016/j.scitotenv.2018.02.341 . hal-04002551

**HAL Id: hal-04002551**

**<https://hal.science/hal-04002551>**

Submitted on 24 Feb 2023

**HAL** is a multi-disciplinary open access archive for the deposit and dissemination of scientific research documents, whether they are published or not. The documents may come from teaching and research institutions in France or abroad, or from public or private research centers.

L'archive ouverte pluridisciplinaire **HAL**, est destinée au dépôt et à la diffusion de documents scientifiques de niveau recherche, publiés ou non, émanant des établissements d'enseignement et de recherche français ou étrangers, des laboratoires publics ou privés.

1 **Seasonal dynamics of transparent exopolymer particles (TEP)**  
2 **and their drivers in the coastal NW Mediterranean Sea**

3 Eva Ortega-Retuerta<sup>1,2,\*</sup>, Ana Muñoz-Fernández<sup>1</sup>, Cèlia Marrasé<sup>1</sup>, M. Montserrat Sala<sup>1</sup>,  
4 Rafel Simó<sup>1</sup>, Josep M Gasol<sup>1</sup>.

5

6 (1) Biologia Marina i Oceanografia, Institut de Ciències del Mar, CSIC, Barcelona,  
7 Catalunya, Spain

8 (2) Sorbonne Université, CNRS, UMR 7621, Laboratoire d'Océanographie  
9 Microbienne, Observatoire Océanologique, Banyuls-sur-Mer, France

10 \*corresponding author [ortegaretuerta@obs-banyuls.fr](mailto:ortegaretuerta@obs-banyuls.fr)

11

12

13 **Abstract**

14           Transparent Exopolymer Particles (TEP) are a subclass of organic particles with  
15 high impact in biogeochemical and ecological processes, such as the biological carbon  
16 pump, air-sea interactions, or the microbial loop. However, the complexity in  
17 production and consumption makes TEP dynamics hardly predictable, calling for the  
18 need of descriptive studies about the in situ dynamics of these particles. We followed  
19 monthly TEP dynamics and combined them with a dataset of environmental variables  
20 during three years in a coastal site of the oligotrophic North Western Mediterranean  
21 (Blanes Bay). TEP concentration, ranging from 11.3 to 289.1  $\mu\text{g XG eq L}^{-1}$  (average  
22  $81.7 \pm 11.7 \mu\text{g XG eq L}^{-1}$ ), showed recurrent peaks in early summer (June-July). TEP  
23 were temporally disconnected from chlorophyll *a* maxima, that occurred in late winter  
24 and early spring (maxima  $1.21 \mu\text{g L}^{-1}$ ), but they were significantly related to the  
25 abundance of specific phytoplankton groups (diatoms and dinoflagellates) and also  
26 coincided with periods of low nutrient concentrations. The fraction of particulate  
27 organic carbon in the form of TEP (the TEP:POC and TEP:PM ratios) were also highest  
28 in early summer, indicating that TEP-enriched particles of low density accumulate in  
29 surface waters during stratified periods. We hypothesize that the accumulation of these  
30 particles affects the microbial food web by enhancing the activity of specific  
31 prokaryotic extracellular enzymes (esterase,  $\beta$ -glucosidase and alkaline phosphatase)  
32 and promoting the abundance of heterotrophic nanoflagellates.

33  
34 **Keywords:** Transparent exopolymer particles, particulate organic carbon,  
35 phytoplankton, prokaryotes, Mediterranean Sea

36  
37

## 1. Introduction

Transparent exopolymer particles (TEP) are operationally defined as acidic polysaccharide particles that are stainable with Alcian Blue (Alldredge et al. 1993). TEP self-assemble from precursors in the dissolved fraction (Zhou et al. 1998) to particles up to hundreds of micrometers, thus spanning the whole dissolved to particulate organic matter continuum (Passow 2002b). Due to their stickiness, TEP promote organic and inorganic particle aggregation forming marine snow, a fundamental process in the biological carbon pump (Passow et al. 1994). However, since TEP have low density, when unballasted they do not sink, and can even ascend in the water column (Azetsu-Scott and Passow 2004) and accumulate in the sea surface microlayer (Wurl et al. 2016). This enrichment affects sea-air fluxes and can be a substantial source of organic aerosols (Aller et al. 2017; Orellana et al. 2011). TEP can also have important impacts on the microbial foodweb: these particles are usually colonized by heterotrophic prokaryotes (Bar-Zeev et al. 2011; Mari and Kiørboe 1996), and the presence of TEP can shape the microbial community as they are preferentially consumed by some prokaryotic groups only (Taylor et al. 2014). In the coastal ocean, the prediction of TEP occurrence has also applied interest since they can be precursors of high mucilage events that affect water quality (Radic et al. 2005; Scoullos et al. 2006), and may clog reverse osmosis membranes in the desalination industry (Berman 2013).

TEP in the ocean are produced mostly by phytoplankton and heterotrophic prokaryotes (Ortega-Retuerta et al. 2010; Passow 2002a). However, in situ TEP dynamics cannot easily be predicted from bulk microbial abundance or activity rates, since not all microbial species produce TEP equally (Passow 2002a, b). In addition, TEP production and formation rates are the result of algal and bacterial physiology state, particularly of nutrient stress (Corzo et al. 2000; Mari et al. 2005) and affected as well by environmental factors such as turbulence (Pedrotti et al. 2010). **TEP sinks, on the other hand, include degradation by photolysis (Ortega-Retuerta et al. 2009) or by prokaryotic enzymatic activity (Smith et al. 1992).** This complexity in production and consumption makes TEP dynamics in the field hardly predictable from one or a few parameters, such as phytoplankton or prokaryote abundance. The lack of simple predictability calls for the collection of data on the dynamics of these particles in situ, particularly throughout full seasonal cycles. Combining TEP observations with a broad suite of physical, chemical and biological measurements should help us understand how these particles are cycled, paving the path for better predictability.

To our knowledge, there are only four previous studies following TEP dynamics over more than one complete seasonal cycle: one in the West coast of India (Bhaskar and Bhosle 2006), one in a freshwater catchment in Southern Spain (Vicente et al. 2009), one in the Fram Strait, Arctic Ocean (Engel et al. 2017) and the fourth one in the coastal North Western Mediterranean (Iuculano et al. 2017). The few other studies describing TEP temporal dynamics in the ocean spanned less than one year or were sampled only occasionally (i.e. two to three times per year (Parinos et al. 2017)), and the observed seasonal patterns did not follow similar trends. For instance, while in some time series TEP and chlorophyll *a* (chl *a*) co-vary (Beauvais et al. 2003; Engel et al. 2017; Parinos et al. 2017; Scoullos et al. 2006), in some others they do not (Bhaskar and Bhosle 2006; Taylor et al. 2014), or they only co-vary at certain periods of the year (Dreshchinskii and Engel 2017).

85 In the NW Mediterranean sea, chl *a* concentration and particulate primary  
86 production are usually highest at the end of the winter (Gasol et al. 2016). During  
87 summer, water stratification enhances nutrient limitation of the prokaryote  
88 communities, mainly due to phosphorus, in surface waters (Pinhassi et al. 2006; Sala et  
89 al. 2002). This nutrient limitation hampers carbon uptake and remineralization  
90 (Thingstad et al. 1997) and thus an accumulation of organic matter from spring to the  
91 end of summer is frequently observed (Romera-Castillo et al. 2013; Vila-Reixach et al.  
92 2012). Aside from studies done in coastal areas that were eutrophic or heavily  
93 influenced by the presence of seagrass meadows, non-representative of the whole  
94 Mediterranean basin (Iuculano et al. 2017; Radic et al. 2005; Scoullou et al. 2006), the  
95 only published study on Mediterranean TEP dynamics (Beauvais et al. 2003) observed  
96 TEP maxima in summer, both at coastal and offshore sites. However, that work  
97 followed only one seasonal cycle, and it is thus not known whether these summer peaks  
98 are recurrent or episodic. A recent study in the Catalan Sea coastal ocean indicated that  
99 horizontal variations of TEP could be predicted from chl *a* concentration only at certain  
100 periods of the year, with higher TEP concentrations respect to chl *a* in summer (Ortega-  
101 Retuerta et al. 2017). Based on these previous studies, we extended our temporal span to  
102 better describe and predict TEP temporal variability. **Our research objective was to**  
103 **explore whether TEP, as an organic carbon pool, would accumulate at the end of**  
104 **summer as other organic moieties do in Blanes Bay, or conversely, as a by-product of**  
105 **plankton activity, would match chl *a* or plankton (both eu- and prokaryote) dynamics.**  
106 We thus followed TEP dynamics combined with a complete dataset of environmental  
107 and biological variables during three years in a coastal site of the North Western  
108 Mediterranean (Blanes Bay). We aimed at solidly describing the annual TEP cycle,  
109 deciphering the main environmental and biological factors that drive TEP variability,  
110 **and exploring the effect of TEP shaping the microbial foodweb. Elucidating the**  
111 **seasonal and interannual TEP recurrence in Mediterranean coastal areas will help to**  
112 **make predictions about their biogeochemical (aerosol formation, particle fluxes) and**  
113 **economical (desalination industry, mucilage formation) effects.**

## 114 **2. Material and methods**

### 115 *2.1. Study site and sampling*

116 Samples were taken from the **long-term** Blanes Bay Microbial Observatory (BBMO).  
117 **This is a well-studied temperate oligotrophic coastal site that has relatively little human**  
118 **or riverine influence (Gasol et al. 2016).** The observatory is located in a shallow (20 m)  
119 open bay (41°39.9'N, 2°48.3'E), around 800 m offshore in the NW **Mediterranean (Fig.**  
120 **1).** **Sampling was performed once per month plus the June solstice from January 2012**  
121 **to October 2014.** In situ temperature-salinity casts were measured using a **calibrated**  
122 **SAIVA/S SD204 sensor. We defined a stratification index as the temperature difference**  
123 **between the surface and near the sea bottom (20 m).** Water transparency was measured  
124 as the Secchi disk depth. Surface (0.5 m) **waters were sampled using a bucket** and pre-  
125 filtered through a 200- $\mu$ m mesh net and kept in the dark in 20-L polycarbonate carboys  
126 until further processing in the lab (within 2 h).

### 127 *2.2. Analytical procedures*

128 TEPs were measured following the colorimetric method proposed by Passow and  
129 Alldredge (1995). Samples (250 mL) were filtered through 25 mm diameter 0.4  $\mu$ m

130 pore size polycarbonate filters (DHI). The filters were stained with 500  $\mu\text{L}$  of pre-  
131 calibrated (with a xanthan gum solution) Alcian Blue (0.02%, pH 2.5) for 5 s and rinsed  
132 with MilliQ water. **Subsequently, they were** soaked in 80% sulfuric acid for 3 h and the  
133 absorbance of the extract was determined at 787 nm in a Varian Cary  
134 spectrophotometer. **The absorption of every batch of Alcian Blue was calibrated using a**  
135 **xanthan gum (XG) solution that was homogenized with a tissue grinder and measured**  
136 **by weight difference.** Duplicates were taken for each sample. **Average SD of duplicates**  
137 **was 8.1, and the detection limit was set to 0.024 absorbance units.** Duplicate blanks  
138 (empty filters stained with Alcian Blue) were also prepared with every batch of filtered  
139 samples. We conducted TEP analyses in formalin-fixed (1% final concentration)  
140 samples, that were preserved at 4°C until filtration (within 3 months at most). We  
141 decided to conduct TEP analyses on fixed samples, since formalin does not interfere  
142 with the measurement (Passow and Alldredge, 1995), in order to optimize the number  
143 of samples processed every time a new calibration curve was constructed (one every  
144 four months). Anyway, we tested for the effect of formalin addition on Alcian Blue  
145 absorption, resulting in non-significant differences between fresh and fixed and stored  
146 samples. **To compare TEP with particulate organic carbon (POC) stocks, we converted**  
147 **TEP into carbon units using the conservative conversion factor of 0.51  $\mu\text{g C } \mu\text{g XG eq}^{-1}$**   
148 **(Engel and Passow 2001)**

149 Chlorophyll *a* concentration (chl *a*) was determined by filtering 150 mL of  
150 seawater on GF/F filters (Whatman), extracting the pigment in acetone (90% v:v) in the  
151 dark at 4°C for 24 h, and measuring fluorescence with a Turner Designs fluorometer.  
152 **Particulate primary production was determined measuring incorporation of  $^{14}\text{CO}_2$  in a**  
153 **light gradient under temperature control. Thirteen 70 ml bottles were inoculated with 10**  
154  **$\mu\text{Ci}$  each and exposed for 2 hours in a light gradient (10-1000  $\mu\text{mol photons m}^{-2} \text{h}^{-1}$ ).**  
155 **The samples were filtered on 0.22  $\mu\text{m}$  cellulose ester filters, exposed to HCl fumes and**  
156 **measured in a liquid scintillation counter. Total in situ production was estimated using**  
157 **the parameters of the P-E curve and the in situ irradiance measured with a Li-Cor**  
158 **sensor.**

159 Analyses of dissolved inorganic nutrient concentrations (nitrate ( $\text{NO}_3$ ), nitrite  
160 ( $\text{NO}_2$ ), ammonium ( $\text{NH}_4$ ) phosphate ( $\text{PO}_4$ ), silicate ( $\text{SiO}_2$ )), were done by standard  
161 segmented flow analyses with colorimetric detection (Hansen and Grasshoff, 1983)  
162 using an SEAL Auto Analyzer AA3 HR. **The detection limits were: 0.0100  $\mu\text{M}$  for**  
163  **$\text{NO}_3$ ; 0.0015  $\mu\text{M}$  for  $\text{NO}_2$ ; 0.0030  $\mu\text{M}$  for  $\text{NH}_4$  (except for 2012, which was 0.0370**  
164  **$\mu\text{M}$ ); 0.0248  $\mu\text{M}$  for  $\text{PO}_4$  and 0.0160  $\mu\text{M}$  for  $\text{SiO}_4$ .** We express dissolved inorganic  
165 nitrogen (DIN) as the sum of  $\text{NO}_3 + \text{NO}_2 + \text{NH}_4$  concentrations. **Samples for particulate**  
166 **matter concentration (PM) were taken only from January 2013 to July 2014 (21 samples**  
167 **in total) and PM was measured** by dry mass weight of 250 mL samples that were  
168 filtered through polycarbonate filters (25 mm diameter, 0.4  $\mu\text{m}$  pore size, DHI) that had  
169 been previously desiccated and weighted. After sample filtration, the filters were dried  
170 for 24 h and weighted again. PM concentration was calculated as the difference in  
171 weight after-before filtration divided by the filtered volume. POC was measured by  
172 filtering 1000 mL of seawater on pre-combusted GF/F glass fiber filters (4 h, 450 °C).  
173 The filters were frozen at -20 °C until analysis. To remove inorganic compounds, prior  
174 to analysis, the filters were thawed in an HCl-saturated atmosphere for 24 h. Then the  
175 filters were dried again and analyzed with a C:H:N autoanalyser (Perkin-Elmer 240).  
176 **The mean values of N and C values for pre-combusted (450°C) GF/F filters were 0.07**  
177  **$\mu\text{mol}$  and 0.53  $\mu\text{mol}$  respectively. These values were subtracted from the values**

178 obtained for each of the samples.

179 Extracellular enzyme activities were quantified with the use of fluorogenic  
180 substrates (Hoppe 1983) according to Sala and Güde (1999) with the modifications for  
181 plate readers described in Sala et al. (2016). Each sample (350  $\mu\text{L}$ ) was pipetted in  
182 quadruplicate into 96 black well plates, with 50  $\mu\text{L}$  of the following substrates: 4-  
183 methylumbelliferyl  $\beta$ -D-glucopyranoside (for  $\beta$ -glucosidase), 4-methylumbelliferyl  
184 phosphate (for alkaline phosphatase), 4-methylumbelliferyl butyrate (for esterase), and  
185 L-leucine-7-amido-4-methyl coumarin (for leu-aminopeptidase). Fluorescence was  
186 measured immediately after addition of the substrate and after incubations of 15 min, 30  
187 min, 1 h, 3 h and 5 h, **in the dark at in situ temperature**. Measurements were done with a  
188 Modulus Microplate (DISMED, Turner BioSystems) at 365 nm emission and 450 nm  
189 excitation wavelengths. The increase of fluorescence units during the period of  
190 incubation was converted into enzymatic activity with a standard curve prepared with  
191 the end products of the reactions, 7-amido-4-methylcoumarin for leu-aminopeptidase  
192 and 4-methylumbelliferone (MUF) for the rest of enzymes.

193 Between 70 mL and 100 mL of glutaraldehyde (1-5% final)-fixed water were filtered  
194 through a 0.6- $\mu\text{m}$  polycarbonate black filter (DHI) and stained with DAPI (Porter and  
195 Feig 1980) to a final concentration of 5 mg mL<sup>-1</sup> to enumerate nanoflagellates by  
196 epifluorescence microscopy (**Olympus BX40, 1000 $\times$** ). In DAPI stained samples,  
197 flagellates presented a bright blue fluorescence under ultraviolet excitation. To  
198 distinguish **pigmented and non-pigmented cells we use blue light excitation, under**  
199 **which Chlorophyll exhibit red fluorescence**. Nanoflagellates showing red fluorescence  
200 **were assumed to be autotrophic and colorless flagellates to be heterotrophic**. **At least 20**  
201 **random fields or 30 cells were counted in each filter**. Bacteria and the different  
202 picophytoplankton organisms were enumerated by flow cytometry following standard  
203 methods after fixation with paraformaldehyde 1% and glutaraldehyde 0.05% (Gasol and  
204 Morán 2016). **Prokaryotic heterotrophic production was estimated from tritiated leucine**  
205 **incorporation in quadruplicate aliquotes and 2 TCA-killed controls to which 40 nM**  
206 **leucine was added**. PHP data are provided as leucine incorporation (pmol leu l<sup>-1</sup> h<sup>-1</sup>).  
207 Microphytoplankton were identified and counted with an inverted microscope after  
208 sedimentation in Utermöhl chambers of formalin- hexamine (0.4% final concentration)  
209 samples kept at 4°C until analysis (Guadayol et al. 2009).

### 210 2.3. Statistical analysis.

211 We checked for statistical differences of the different environmental variables  
212 among seasons using Mann Whitney tests after Bonferroni corrections. **The seasons**  
213 **were separated by the winter/summer solstices and the spring/fall equinoxes**. To assess  
214 co-variability between environmental and biological variables in the Blanes dataset,  
215 pairwise Spearman Rank correlation analyses were performed, and seasonality was  
216 tested by autocorrelation analysis using the PAST software (Hammer 2001). The level  
217 of significance (p) was set at 0.05. Principal component analysis (*Stats* and *ggfortify*  
218 packages in R), was applied to all samples after centering and scaling a total number of  
219 25 physical, chemical and biological variables.

## 220 3. Results

221

### 222 3.1. Variation of the main physical and chemical parameters in Blanes Bay

223 As the heat flux and seawater temperature rise in summer, the establishment of a  
224 stratified layer is frequently observed, as illustrated by significant increases in the  
225 stratification index (Table 1). Consequently, surface nutrients normally exhibit lower  
226 concentrations in summer (Guadayol et al. 2009). **In the studied three-year period,**  
227 dissolved phosphate (DIP) concentration varied between 0.03 and 0.22  $\mu\text{mol L}^{-1}$ ,  
228 dissolved inorganic nitrogen (DIN) ranged from **0.29 to 5.35  $\mu\text{mol L}^{-1}$**  and silicate  
229 varied between 0.46 and 2.49  $\mu\text{mol L}^{-1}$  (Table 1). **DIN and silicate were significantly**  
230 **lower in summer than in winter (Table 1), but no significant differences in DIP between**  
231 **seasons were observed.** Water transparency, measured as Secchi disk depths, ranged  
232 between 8 and 20 m (Table 1).

### 233 3.2. Seasonal variability of TEP and other particle stocks in Blanes Bay

234 In that three-year period, TEP ranged from 11.3 to 289.1  $\mu\text{g XG eq L}^{-1}$  (average  
235  $81.7 \pm 11.7 \mu\text{g XG eq L}^{-1}$ ). The highest concentrations of TEP were recurrently  
236 observed in early summer (June solstice and July, average  $224.0 \pm 7.9 \mu\text{g XG eq L}^{-1}$ ,  
237 Fig. 2a). After the early summer peak, TEP concentrations decreased again, reaching  
238 minimum values in the fall and winter (Fig. 2a). This pattern was interannually  
239 recurrent with a lag= 13, corresponding to thirteen samples per year (**two sampling**  
240 **times in June; autocorrelation analysis,  $r = 0.79$ ,  $p < 0.05$** ). However, the early summer  
241 peak **magnitude** was highest in 2012 (more than 250  $\mu\text{g XG eq L}^{-1}$  in the June solstice  
242 and July, Fig. 2a). By contrast, TEP in late summer (August and September) were  
243 highest in 2014 (192.0  $\mu\text{g XG eq L}^{-1}$ , Fig. 2a).

244 Particulate matter concentration (PM) ranged from 0.162 to 0.852  $\text{mg L}^{-1}$   
245 (average  $0.417 \pm 0.199 \text{mg L}^{-1}$ ). Maxima were recorded in the winter months  
246 (December to March) and the June solstice (Fig. 2b). Particulate organic carbon (POC)  
247 concentrations ranged from 5.43 to 23.95  $\mu\text{mol L}^{-1}$  (average  $9.73 \pm 4.61 \mu\text{mol L}^{-1}$ ).  
248 POC concentrations did not follow the same seasonal pattern throughout the three study  
249 years (Fig. 2b), hence they did not show significant differences over the year (Table 1).  
250 TEP, PM and POC dynamics were not significantly coupled (Table 2). However, PM,  
251 as expected, was negatively correlated to water transparency ( $r = -0.53$ ,  $p < 0.02$ ,  $n =$   
252 19). The TEP/PM and TEP/POC ratios progressively increased from winter to summer,  
253 decreasing again in the fall (Fig. 2c).

### 254 3.3. Seasonal variability of biological parameters in Blanes Bay

255 Chlorophyll *a* (chl *a*) ranged from 0.15 to 1.21  $\mu\text{g L}^{-1}$ . Maxima of chl *a* occurred  
256 **in March 2012 and 2013**; but in 2014 the maximum was in January-February (Fig. 3a).  
257 The dynamics of chl *a* were not significantly correlated to variations of single  
258 phytoplankton groups (diatoms, coccolithophorids, cryptophytes, cyanobacteria).  
259 *Synechococcus* presented peaks of high abundance in April 2012 and 2013, but not in  
260 2014, when the highest abundances were recorded in late summer (Fig. 3b). The  
261 abundances of *Prochlorococcus* cells were always highest in fall (Fig. 3b). Pico- and  
262 nanoplankton abundances were highest in the first 4 months of every year, although a  
263 second period of relatively high nanoeukaryote abundance was also apparent in May-  
264 June 2014 (Fig. 3c). Dinoflagellates and diatoms showed abundance peaks in June-July  
265 2012 and 2013, and in **August**, only for dinoflagellates, in 2014 (Fig. 3d). The  
266 abundance of coccolithophorids and other microplankton groups did not exhibit clear  
267 seasonal variations in the form of recurrent peaks (Fig. 3e). Primary production,

268 determined once per season, ranged from 0.58 to 1.63 mg m<sup>-3</sup> h<sup>-1</sup> and was highest,  
269 although not significant, in spring (1.16 mg m<sup>-3</sup> h<sup>-1</sup>), but the maximum value was  
270 recorded in September 2013.

271 Prokaryotic heterotrophic abundance (PHA) ranged from 4.4 to 14.4 x10<sup>5</sup> cell  
272 mL<sup>-1</sup> (Fig. 4a). Prokaryotic heterotrophic production (PHP) ranged from 3.6 to 364.4  
273 pmol leu L<sup>-1</sup> h<sup>-1</sup> (equivalent to 0.13 to 13.56 µgC L<sup>-1</sup> d<sup>-1</sup>, Fig. 4a). PHA was  
274 significantly lower in the winter than in the rest of the seasons, while PHP was  
275 significantly higher in summer than in winter (Table 1). The activities of the  
276 exoenzymes alkaline phosphatase and esterase were significantly higher in summer  
277 (Table 1, Fig. 4b-c). The activity of β-Glucosidase was highest in summer (Fig. 4d), yet  
278 not statistically significant, and Leucine aminopeptidase activity was highest in spring  
279 (Table 1). The abundances of heterotrophic flagellates, ranging from 210 to 2718 cells  
280 mL<sup>-1</sup>, were significantly higher in summer than in the rest of seasons (Table 1).

### 281 3.4. Environmental and biological variables *determining* TEP dynamics in Blanes Bay

282 Higher TEP concentrations were found in early summer. Therefore, TEP co-  
283 varied with sea surface temperature and the stratification index (Table 2). The dynamics  
284 of TEP and chl *a* were not significantly coupled (Table 2). Rather, cross-correlation  
285 analyses showed a lag-time of 4 months between chl *a* and TEP peaks ( $r = 0.48$ ,  $p <$   
286  $0.04$ ). TEP were significantly related to the abundance of specific phytoplankton  
287 groups, such as diatoms ( $r = 0.63$   $p < 0.001$ ,  $n=33$ ) and dinoflagellates ( $r = 0.65$   $p <$   
288  $0.001$ ,  $n=33$ ). No significant correlations were found between TEP and other eukaryotic  
289 (coccolithophores, cryptophytes) nor prokaryotic (*Synechococcus* and *Prochlorococcus*)  
290 groups (Table 2).

291 Non-significant covariations were observed between TEP and PHA and PHP  
292 (Fig. 4a-b). Noticeably, increases in TEP coincided with increases in some extracellular  
293 enzyme activities: Esterase ( $r = 0.60$   $p < 0.001$ ,  $n=34$ ), alkaline phosphatase ( $r = 0.66$   $p$   
294  $< 0.001$ ,  $n=34$ ), β-glucosidase ( $r = 0.69$   $p < 0.001$ ,  $n=34$ , Table 2). TEP were also  
295 significantly correlated to the abundance of heterotrophic nanoflagellates (Table 2).

296 A principal component analysis (PCA) was performed to visualize which subset  
297 of variables could better explain the TEP seasonal patterns in Blanes Bay. Principal  
298 components 1 and 2 explained 29.0 and 13.2% of the variability respectively.  
299 Component 1 separated the data between summer and winter samples (Fig. 5) and the  
300 major loadings included temperature (0.32), stratification index (0.30), TEP  
301 concentration (0.31) and (negatively related) dissolved inorganic silica (Si; -0.32) and  
302 nitrogen (DIN; -0.29). Component 2 separated the samples along a productivity  
303 gradient, where the major loadings included chl *a* (-0.33), diatoms (-0.33) and  
304 dinoflagellates (-0.35) and prokaryotic heterotrophic production (PHP, 0.33). Early  
305 summer samples clustered together since they had relatively high stratification indices,  
306 TEP and POC concentrations, heterotrophic nanoflagellates (HNF), and abundance of  
307 diatoms, dinoflagellates and other microphytoplankton groups (Fig. 5).

## 308 4. Discussion

309 To date, and as we are aware, there are only three published seasonal studies on  
310 TEP variability in the Mediterranean Sea (Beauvais et al. 2003; Iuculano et al. 2017;

311 Mari et al. 2001). In Mari et al. (2001) and Beauvais et al. (2003), that present the same  
312 12-month TEP data series, TEP accumulation was observed in June in offshore and  
313 coastal sites. However, absolute values cannot be compared since TEP were quantified  
314 using different methods (microscopic enumeration in their study vs. colorimetric assay  
315 in ours). Chl *a* was also highest in June at the deep chlorophyll maxima in the offshore  
316 site, yielding a significant correlation with TEP abundance. Conversely, chl *a* in their  
317 coastal site was highest in March but TEP peaks occurred in early summer, thus TEP  
318 and chl *a* seemed to be decoupled as in our study. In the Balearic Sea, TEP ranges were  
319 similar to our study (from 4.6 to 90.6  $\mu\text{g XG eq L}^{-1}$ ) in a rocky shore coastal site  
320 (Iuculano et al. 2017), while higher TEP concentrations were found in a coastal site  
321 accumulating *Posidonia oceanica* leaf litter (from 26.8 to 1878.4  $\mu\text{g XG eq L}^{-1}$ ). Our  
322 detailed three-year seasonal study showed, in accordance with these previous studies,  
323 that TEP accumulation in surface waters of the coastal NW Mediterranean Sea is a  
324 recurring pattern in early summer, but not in late summer as occurs with other organic  
325 matter pools (Romera-Castillo et al. 2013; Vila-Reixach et al. 2012). Other temporal  
326 studies in the Mediterranean Sea (Parinos et al. 2017; Radic et al. 2005; Scoullos et al.  
327 2006) have lower temporal resolution (i.e. 3 times per year, (Parinos et al. 2017)) or had  
328 been performed in quite more eutrophic areas (i.e. the Aegean Sea and the Northern  
329 Adriatic Sea at the Po River delta). Parinos et al. (2017) showed in the Aegean Sea  
330 surface, contrary to our results, higher TEP in March ( $101 \pm 32.7 \mu\text{g XG eq L}^{-1}$ ) than in  
331 July ( $88.6 \pm 26.5 \mu\text{g XG eq L}^{-1}$ ). (Radic et al. 2005; Scoullos et al. 2006) show high  
332 interannual TEP variations in eutrophic coastal areas in the Adriatic and Aegean Seas.  
333 The few other time series studies in marine ecosystems (i.e. Engel et al. (2017) in the  
334 Arctic Ocean, Klein et al. (2011) and Taylor et al. (2014) in the English Channel,  
335 Bhaskar and Bhosle (2006) in the West coast of India) are climatically and  
336 oceanographically very different from, hence hardly comparable to, our temperate  
337 oligotrophic coastal system.

338 Ocean particles often contain a variable proportion of TEP or gel-like structures. The  
339 proportion of TEP vs. POC or vs. solid particles determines their export efficiency  
340 (Azetsu-Scott and Passow 2004; Mari et al. 2017). Particles with high TEP content have  
341 lower density than those not enriched in TEP (Mari et al. 2017), and thus have higher  
342 retention times in the water column. Comparison between ours and previous studies that  
343 calculated the proportion of TEP to PM is not possible, since different methodologies  
344 (and thus particle fractions) have been employed (dry weight onto 0.4  $\mu\text{m}$  filters in our  
345 case, particle volume fractions determined by Coulter counter in Engel (2004) and  
346 Prieto et al. (2006)). In our study, TEP and other particles, either POC or total particle  
347 mass (PM), were decoupled. Particles in early summer showed the highest TEP:PM  
348 ratio, indicating that the particle stocks were mainly composed by low density particles  
349 that are less efficiently exported, thus weakening organic carbon sinking fluxes.

350 Comparing the TEP and POC pools in our dataset, we observed that in early summer  
351 TEP represented on average 77% of POC (Fig. 2c). We used the most conservative  
352 conversion factor, this is,  $0.51 \mu\text{g C } \mu\text{g XG eq}^{-1}$ , from those proposed by Engel and  
353 Passow (2001), which would correspond to diatom-dominated ecosystems. While it  
354 could be a good proxy for our early summer data, we may be over- or underestimating  
355 the TEP-C pool in other periods of the year. Also, previous studies in the Mediterranean  
356 Sea (Bar-Zeev et al. 2011; Ortega-Retuerta et al. 2010) using the published conversion  
357 factors show higher TEP-C than POC, which is obviously inaccurate and claim for the  
358 need to determine specific conversion factors to convert TEP in C units in this area. We  
359 are aware about the shortcomings of conversion factors, however we consider that for  
360 the purpose of our study, the interannual variability of TEP throughout the years, the

361 Engel and Passow (2001) conversion factor, used here, is appropriate to estimate such  
362 variability. TEP can accumulate in the water column during several months (Mari et al.  
363 2017), and get trapped and enriched near the surface by strengthening stratification.  
364 Although no previous studies have considered TEP when looking at particle dynamics  
365 in Blanes, López-Fernández et al. (2013) observed that the organic carbon content of the  
366 particles in the nearby Blanes canyon was also highest in summer, although particle  
367 fluxes were higher in winter.

368 The comparison of TEP dynamics with a complete suite of environmental and  
369 biological variables highlighted the complexity of predicting TEP occurrence based on  
370 few parameters. In fact, correlation analyses revealed that only up to 48% of the  
371 variance of TEP can be explained by a single parameter (Table 2). In addition, only  
372 40% of the overall variation in Blanes Bay samples was explained by the available data  
373 as indicated from the PCA. Based on our observation that TEP did not correlate to  
374 prokaryote abundance nor production, we suggest that phytoplankton rather than  
375 prokaryotes are the main TEP source in Blanes Bay. Indeed, TEP were significantly  
376 correlated to the abundance of diatoms and dinoflagellates, that are known to produce  
377 TEP (Passow 2002b) and references therein. If TEP in Blanes Bay are a direct result of  
378 the presence of these groups, we can predict that TEP maxima will normally occur in  
379 spring, when these phytoplankton groups usually peak (Nunes et. al. submitted). Longer  
380 time series would be necessary to explore this hypothesis further. However, we  
381 observed summer TEP accumulation also in July 2014, when relevant increases in  
382 diatoms or dinoflagellates were not detected (only a peak of dinoflagellates was  
383 detected in August, Fig. 2d). Therefore, we argue that release by phytoplankton cannot  
384 be the only factor determining the presence of TEP peaks in Blanes Bay.

385 Nutrient limitation enhances TEP production rates (Corzo et al. 2000), making  
386 TEP concentrations higher in the summer months when nutrients are scarcer. The lag-  
387 phase observed between chl *a* and TEP peaks in Blanes Bay would concur with  
388 previous results that suggest that TEP production is normally higher at the end of  
389 phytoplankton blooms when nutrients have been exhausted rather than at maximum chl  
390 *a* levels (Engel 2000; Hong et al. 1997). After the chl *a* peak, TEP would accumulate in  
391 early summer assisted by the increasing stratification, that prevents vertical export and  
392 further injections of nutrients from below (higher nutrient concentration increases with  
393 depth in summer (Aparicio et al. 2017)). In other words, TEP would result from the  
394 combination of high chl *a* values in late winter, evolving nutrient limitation from spring  
395 on, and stronger stratification in summer, when significantly lower nitrogen  
396 concentrations were found (Table 1). This is particularly noticeable in 2014, when TEP  
397 peaks were not concurrent with high abundance of diatoms but DIN and silicate  
398 concentration showed low values ( $0.39 \mu\text{mol L}^{-1}$ , the lowest value for the entire period),  
399 which would enhance per cell TEP production by phytoplankton. The joint effects of  
400 these processes would explain TEP dynamics in the area. More studies (e.g., with  
401 controlled incubations) to quantify TEP production and consumption in different  
402 seasons and/or nutrient levels are needed to validate this hypothesis.

403 Once TEP have accumulated at the surface in early summer, they can serve as a  
404 substrate for further processing by the microbial communities. In our dataset, TEP were  
405 not related to heterotrophic prokaryote abundance nor production, so here we discard a  
406 major source of TEP from prokaryotes. However, TEP were correlated to the activities  
407 of specific enzymes ( $\beta$ -glucosidase, esterase and alkaline phosphatase); thus, TEP likely

408 shaped prokaryote functional diversity although not bulk abundances nor biomass  
409 production. High enzymatic activity associated to marine aggregates has been  
410 previously shown (Smith et al. 1992). As TEP are mainly composed of acidic  
411 polysaccharide (Passow 2002b), we could hypothesize that TEP maxima would be  
412 followed by higher increases in enzymes involved in the degradation of these  
413 substances (i.e.  $\beta$ -glucosidase and esterase) than in aminopeptidase or phosphatase  
414 enzymes. This was confirmed by the correlation between TEP and  $\beta$ -glucosidase and  
415 esterase. Looking back in the Blanes Bay time series, we observed that  $\beta$ -glucosidase  
416 activities recurrently peak in summer (Alonso-Sáez et al. 2008). Although this relation  
417 is not surprising since TEP are carbon-rich substances, the effect of TEP accumulation  
418 on specific microbial metabolisms is worthy to note. Similar positive correlations  
419 between TEP and  $\beta$ -glucosidase had previously been observed in controlled incubations  
420 using Eastern Mediterranean waters (Rahav et al. 2016) but not in a time series in the  
421 west coast of India (Bhaskar and Bhosle 2006). No previous studies have compared  
422 TEP concentration and esterase activities, but TEP are made of polysaccharides  
423 enriched in sulfate in the form of half-ester groups (Passow and Alldredge 1995) being  
424 thus likely the coincidence between TEP peaks and high esterase activity. Increases in  
425 TEP were also concurrent with increases in the activities of alkaline phosphatase. This  
426 has previously been shown in the Eastern Mediterranean basin (Bar-Zeev et al. 2011)  
427 and in controlled experiments (Berman-Frank et al. 2016). Prokaryotic abundance and  
428 activity in Blanes Bay in summer is controlled by the availability of inorganic  
429 phosphorus (Pinhassi et al. 2006), although we did not observe significant decreases in  
430 P in summer in our study years (Table 1). Previous studies have suggested that under  
431 phosphorus limitation, prokaryotes could use alkaline phosphatase to access phosphorus  
432 from alternative sources such as TEP (Berman-Frank et al. 2016). However, to our  
433 knowledge, TEP are not directly enriched in phosphorus (although phosphorus  
434 compounds could be adsorbed into the gel-like TEP structure). In addition, lower N/P  
435 ratios in summer suggest, contrary to previous knowledge (Sala et al 2002, Pinhassi et  
436 al. 2006), that P was not the limiting nutrient for prokaryotes in Blanes Bay. We cannot  
437 rule out with our approach the possibility that increases in enzyme activities are not a  
438 direct consequence of the presence of TEP but both factors increase concurrently due to  
439 the release of specific DOM compounds by phytoplankton during periods of high  
440 phosphorus limitation. Experimental studies with manipulations of the environmental  
441 conditions or time series studies with higher resolution would be needed to sort this out.

442 After TEP maxima in early summer, TEP peaks decreased to reach lower values  
443 at the end of summer. Based on our results, TEP decreases after summer peaks could be  
444 a direct consequence of this extracellular enzyme activities. Other non-exclusive sinks  
445 that likely accounted for TEP decreases is photolysis, which can degrade TEP stocks in  
446 few days (Ortega-Retuerta et al. 2009), as TEP maxima in our study, coincide with  
447 longer days and highest solar radiation (Ruiz-González et al. 2012). Finally, we cannot  
448 rule out the possibility that TEP are exported to deeper layers at the end of summer  
449 when waters become less stratified. Also, the high stickiness of TEP-rich material  
450 (Engel 2000) favours the particle aggregation thus facilitating its export

451 TEP dynamics in Blanes Bay also co-varied with the abundance of heterotrophic  
452 nanoflagellates. These covariations were also observed by Arnous et al. (2010) in a  
453 lake, where TEP and PHA were not correlated either. Since the prokaryote to  
454 heterotrophic nanoflagellate ratios in Blanes Bay are lowest in early summer (data not  
455 shown), these organisms could benefit from feeding on TEP-attached prokaryotic

456 communities, which are believed to occur at higher densities than their free-living  
457 counterparts. Although prokaryote colonization of TEP was not directly measured in  
458 our study, higher densities of prokaryotic cells on TEP than in the surrounding water  
459 have been repeatedly observed (Bar-Zeev et al. 2011; Mari and Kiørboe 1996). An  
460 alternative non-excluding explanation is that heterotrophic nanoflagellates embedded in  
461 the TEP matrix are protected against predation by ciliates and microzooplankton  
462 (Arnous et al. 2010).

## 463 Conclusions

464 We have confirmed the seasonal recurrence of TEP in the oligotrophic North  
465 Western Mediterranean Sea and the temporal disconnection between TEP and  
466 chlorophyll *a* in a three-year dataset. **We present evidence that the TEP dynamics result  
467 from a combination of factors rather than from the variation of a single predictor  
468 variable. The presence of specific phytoplankton groups (diatoms and dinoflagellates),  
469 the possible enhancement of TEP production under nutrient limitation, the TEP  
470 accumulation at surface due to positive buoyancy (low density) and the water  
471 stratification would give rise to TEP maxima in early summer.** We hypothesize that the  
472 presence of these particles has an effect in the microbial food web by enhancing the  
473 activity of specific prokaryotic extracellular enzymes and likely promoting the  
474 abundance of heterotrophic nanoflagellates.

## 475 5. Acknowledgements

476 This work was funded by projects STORM (CTM2009-09352/MAR), PEGASO  
477 (CTM2012-37615), ANIMA (CTM2015-65720-R) and REMEI (CTM2015-70340-R)  
478 of the Spanish Ministry of Science or Economy. Thanks to all the Blanes team, in  
479 particular Clara Cardelús and Vanessa Balagué, for their organization and sampling  
480 efforts, and Ramon Massana and Encarna Borrell for providing heterotrophic  
481 nanoflagellate and enzyme activities data. Marina Zamanillo helped with TEP  
482 measurements. EOR was supported by a Juan de la Cierva fellowship. We thank six  
483 anonymous reviewers for their supportive comments that helped improve the MS

## 484 6. References

- 485 Alldredge, A.L., Passow, U., & Logan, B.E. (1993). The abundance and significance of  
486 a class of large, transparent organic particles in the ocean. *Deep Sea Research I*, 40,  
487 1131-1140
- 488 Aller, J.Y., Radway, J.C., Kiltath, W.P., Bothe, D.W., Wilson, T.W., Vaillancourt,  
489 R.D., Quinn, P.K., Coffman, D.J., Murray, B.J., & Knopf, D.A. (2017). Size-resolved  
490 characterization of the polysaccharidic and proteinaceous components of sea spray  
491 aerosol. *Atmospheric Environment*, 154, 331-347
- 492 Alonso-Sáez, L., Vázquez-Domínguez, E., Cardelús, C., Pinhassi, J., Sala, M.M.,  
493 Lekunberri, I., Balagué, V., Vila-Costa, M., Unrein, F., Massana, R., Simó, R., & Gasol,  
494 J.M. (2008). Factors controlling the year-round variability in carbon flux through  
495 bacteria in a coastal marine system. *Ecosystems*, 11, 397-409
- 496 Aparicio, F.L., Nieto-Cid, M., Calvo, E., Pelejero, C., López-Sanz, À., Pascual, J.,  
497 Salat, J., Sánchez-Pérez, E.D., La Fuente, P.D., Gasol, J.M., & Marrasé, C. (2017).  
498 Wind-induced changes in the dynamics of fluorescent organic matter in the coastal NW  
499 Mediterranean. *Science of the Total Environment*, 609, 1001-1012

500 Arnous, M.-B., Courcol, N., & Carrias, J.-F. (2010). The significance of transparent  
501 exopolymeric particles in the vertical distribution of bacteria and heterotrophic  
502 nanoflagellates in Lake Pavin. *Aquatic Sciences*, 72, 245-253

503 Azetsu-Scott, K., & Passow, U. (2004). Ascending marine particles: Significance of  
504 transparent exopolymer particles (TEP) in the upper ocean. *Limnology and  
505 Oceanography*, 49, 741-748

506 Bar-Zeev, E., Berman, T., Rahav, E., Dishon, G., Herut, B., Kress, N., & Berman-  
507 Frank, I. (2011). Transparent exopolymer particle (TEP) dynamics in the eastern  
508 Mediterranean Sea. *Marine Ecology-Progress Series*, 431, 107-118

509 Beauvais, S., Pedrotti, M.L., Villa, E., & Lemée, R. (2003). Transparent exopolymer  
510 particle (TEP) dynamics in relation to trophic and hydrological conditions in the NW  
511 Mediterranean Sea. *Mar Ecol Progr Ser*, 262, 97-109

512 Berman, T. (2013). Transparent exopolymer particles as critical agents in aquatic  
513 biofilm formation: implications for desalination and water treatment. *Desalination and  
514 Water Treatment*, 51, 1014-1020

515 Berman-Frank, I., Spungin, D., Rahav, E., Van Wambeke, F., Turk-Kubo, K., &  
516 Moutin, T. (2016). Dynamics of transparent exopolymer particles (TEP) during the  
517 VAHINE mesocosm experiment in the New Caledonian lagoon. *Biogeosciences*, 13,  
518 3793-3805

519 Bhaskar, P.V., & Bhosle, N.B. (2006). Dynamics of transparent exopolymeric particles  
520 (TEP) and particle-associated carbohydrates in the Dona Paula bay, west coast of India.  
521 *Journal of Earth System Science*, 115, 403-413

522 Corzo, A., Morillo, J.A., & Rodríguez, S. (2000). Production of transparent exopolymer  
523 particles (TEP) in cultures of *Chaetoceros calcitrans* under nitrogen limitation. *Mar  
524 Ecol Progr Ser*, 23, 63-72

525 Dreshchinskii, A., & Engel, A. (2017). Seasonal variations of the sea surface microlayer  
526 at the Boknis Eck Times Series Station (Baltic Sea). *Journal of Plankton Research*, 1-  
527 19

528 Engel, A. (2000). The role of transparent exopolymer particles (TEP) in the increase in  
529 apparent particle stickiness ( $\alpha$ ) during the decline of a diatom bloom. *Journal of  
530 Plankton Research*, 22, 485-497

531 Engel, A. (2004). Distribution of transparent exopolymer particles (TEP) in the  
532 northeast Atlantic Ocean and their potential significance for aggregation processes.  
533 *Deep Sea Research Part I: Oceanographic Research Papers*, 51, 83-92

534 Engel, A., & Passow, U. (2001). Carbon and nitrogen content of transparent  
535 exopolymer particles (TEP) in relation to their Alcian Blue adsorption. *Mar. Ecol. Prog  
536 Ser.*, 219, 1-10

537 Engel, A., Piontek, J., Metfies, K., Endres, S., Sprong, P., Peeken, I., Gabler-Schwarz,  
538 S., & Nothig, E.M. (2017). Inter-annual variability of transparent exopolymer particles  
539 in the Arctic Ocean reveals high sensitivity to ecosystem changes. *Sci Rep*, 7, 4129

540 Gasol, J.M., Cardelús, C., Morán, X.A.G., Balagué, V., Massana, R., Pedrós-Alió, C.,  
541 Sala, M.M., Simó, R., Vaqué, D., & Estrada, M. (2016). Seasonal patterns in  
542 phytoplankton photosynthetic parameters and primary production in a coastal NW  
543 Mediterranean site. *Sci. Mar.*, *In press*

544 Gasol, J.M., & Morán, X.A.G. (2016). Flow Cytometric Determination of Microbial  
545 Abundances and Its Use to Obtain Indices of Community Structure and Relative  
546 Activity. In T.J. McGenity, K.N. Timmis, & B. Nogales (Eds.), *Hydrocarbon and Lipid  
547 Microbiology Protocols: Single-Cell and Single-Molecule Methods* (pp. 159-187).  
548 Berlin, Heidelberg: Springer Berlin Heidelberg

549 Guadayol, O., Marrasé, C., Peters, F., Berdalet, E., Roldá, N., & Sabata, A. (2009).  
550 Responses of coastal osmotrophic planktonic communities to simulated events of  
551 turbulence and nutrient load throughout a year. *Journal of Plankton Research*, *31*, 583-  
552 600

553 Hammer, Ø., Harper, D.A.T., Ryan, P.D. (2001). PAST: Paleontological statistics  
554 software package for education and data analysis. . *Palaeontologia Electronica* *4*(1):  
555 9pp.

556 Hong, Y., Smith Jr, W.O., & White, A.M. (1997). Studies on transparent exopolymer  
557 particles (TEP) produced in the ross sea (Antarctica) and by *Phaeocystis antarctica*  
558 (*Prymnesiophyceae*). *Journal of Phycology*, *33*, 368-376

559 Hoppe, H.G. (1983). Significance of exoenzymatic activities in the ecology of brackish  
560 water: measurements by means of methylumbelliferyl substrates. *Mar Ecol Progr Ser*,  
561 *11*, 299-308

562 Iuculano, F., Duarte, C.M., Marbà, N., & Agustí, S. (2017). Seagrass as major source  
563 of transparent exopolymer particles in the oligotrophic Mediterranean coast.  
564 *Biogeosciences Discussions*, 1-12

565 Klein, C., Claquin, P., Pannard, A., Napoléon, C., Le Roy, B., & Véron, B. (2011).  
566 Dynamics of soluble extracellular polymeric substances and transparent exopolymer  
567 particle pools in coastal ecosystems. *Marine Ecology Progress Series*, *427*, 13-27

568 López-Fernández, P., Bianchelli, S., Pusceddu, A., Calafat, A., Sanchez-Vidal, A., &  
569 Danovaro, R. (2013). Bioavailability of sinking organic matter in the Blanes canyon and  
570 the adjacent open slope (NW Mediterranean Sea). *Biogeosciences*, *10*, 3405-3420

571 Mari, X., Beauvais, S., Lemée, R., & Pedrotti, M.L. (2001). Non-Redfield C : N ratio of  
572 transparent exopolymeric particles in the northwestern Mediterranean Sea. *Limnology*  
573 *and Oceanography*, *46*, 1831-1836

574 Mari, X., & Kjørboe, T. (1996). Abundance, size distribution and bacterial colonization  
575 of transparent exopolymeric particles (TEP) during spring in the Kattegat. *Journal of*  
576 *Plankton Research*, *18*, 969-986

577 Mari, X., Passow, U., Migon, C., Burd, A.B., & Legendre, L. (2017). Transparent  
578 exopolymer particles: Effects on carbon cycling in the ocean. *Progress in*  
579 *Oceanography*, *151*, 13-37

580 Mari, X., Rassoulzadegan, F., Brussaard, C.P.D., & Wassmann, P. (2005). Dynamics of  
581 transparent exopolymeric particles (TEP) production by *Phaeocystis globosa* under N-  
582 or P-limitation: a controlling factor of the retention/export balance. *Harmful Algae*, *4*,  
583 895-914

584 Orellana, M.V., Matrai, P.A., Leck, C., Rauschenberg, C.D., Lee, A.M., & Coz, E.  
585 (2011). Marine microgels as a source of cloud condensation nuclei in the high Arctic.  
586 *Proceedings of the National Academy of Sciences*, *108*, 13612-13617

587 Ortega-Retuerta, E., Duarte, C.M., & Reche, I. (2010). Significance of Bacterial  
588 Activity for the Distribution and Dynamics of Transparent Exopolymer Particles in the  
589 Mediterranean Sea. *Microbial Ecology*, *59*, 808-818

590 Ortega-Retuerta, E., Passow, U., Duarte, C.M., & Reche, I. (2009). Effects of ultraviolet  
591 B radiation on (not so) transparent exopolymer particles. *Biogeosciences*, *6*, 3071-3080

592 Ortega-Retuerta, E., Sala, M.M., Mestre, M., Borrull, E., Marrasé, C., Aparicio, F.L.,  
593 Gallisai, R., Antequera, C., Peters, F., Simó, R., & Gasol, J.M. (2017). Horizontal and  
594 vertical distributions of Transparent exopolymer particles (TEP) in the NW  
595 Mediterranean Sea are linked to chlorophyll a and O<sub>2</sub> variability. *Frontiers in*  
596 *Microbiology*, *in press*

597 Parinos, C., Gogou, A., Krasakopoulou, E., Lagaria, A., Giannakourou, A.,  
598 Karageorgis, A.P., & Psarra, S. (2017). Transparent Exopolymer Particles (TEP) in the

599 NE Aegean Sea frontal area: Seasonal dynamics under the influence of Black Sea water.  
600 *Continental Shelf Research*

601 Passow, U. (2002a). Production of transparent exopolymer particles (TEP) by phyto-  
602 and bacterioplankton. *Marine Ecology Progress Series*, 236, 1-12

603 Passow, U. (2002b). Transparent exopolymer particles (TEP) in aquatic environments.  
604 *Progress in Oceanography*, 55, 287-333

605 Passow, U., & Alldredge, A.L. (1995). A dye-binding assay for the spectrophotometric  
606 measurement of transparent exopolymer particles (TEP). *Limnology and*  
607 *Oceanography*, 40, 1326-1335

608 Passow, U., Alldredge, A.L., & Logan, B.E. (1994). The role of particulate  
609 carbohydrate exudates in the flocculation of diatom blooms. *Deep Sea Res. I*, 41, 335-  
610 357

611 Pedrotti, M.L., Peters, F., Beauvais, S., Vidal, M., Egge, J., Jacobsen, A., & Marrasé, C.  
612 (2010). Effects of nutrients and turbulence on the production of transparent exopolymer  
613 particles: A mesocosm study. *Marine Ecology Progress Series*, 419, 57-69

614 Pinhassi, J., Gomez-Consarnau, L., Alonso-Sáez, L., Sala, M.M., Vidal, M., Pedrós-  
615 Alió, C., & Gasol, J.M. (2006). Seasonal changes in bacterioplankton nutrient limitation  
616 and their effects on bacterial community composition in the NW Mediterranean Sea.  
617 *Aquatic Microbial Ecology*, 44, 241-252

618 Porter, K.G., & Feig, Y.S. (1980). The use of DAPI for identifying and counting aquatic  
619 microflora. *Limnology and Oceanography*, 25, 943-948

620 Prieto, L., Navarro, G., Cózar, A., Echevarría, F., & García, C.M. (2006). Distribution  
621 of TEP in the euphotic and upper mesopelagic zones of the southern Iberian coasts.  
622 *Deep Sea Research Part II: Topical Studies in Oceanography*, 53, 1314-1328

623 Radic, T., Kraus, R., Fuks, D., Radic, J., & Pecar, O. (2005). Transparent exopolymeric  
624 particles' distribution in the northern Adriatic and their relation to microphytoplankton  
625 biomass and composition. *Science of the Total Environment*, 353, 151-161

626 Rahav, E., Giannetto, M.J., & Bar-Zeev, E. (2016). Contribution of mono and  
627 polysaccharides to heterotrophic N<sub>2</sub> fixation at the eastern Mediterranean coastline. *Sci*  
628 *Rep*, 6, 27858

629 Romera-Castillo, C., Álvarez-Salgado, X.A., Galí, M., Gasol, J.M., & Marrasé, C.  
630 (2013). Combined effect of light exposure and microbial activity on distinct dissolved  
631 organic matter pools. A seasonal field study in an oligotrophic coastal system (Blares  
632 Bay, NW Mediterranean). *Marine Chemistry*, 148, 44-51

633 Ruiz-González, C., Lefort, T., Galí, M., Montserrat Sala, M., Sommaruga, R., Simó, R.,  
634 & Gasol, J.M. (2012). Seasonal patterns in the sunlight sensitivity of bacterioplankton  
635 from Mediterranean surface coastal waters. *Fems Microbiology Ecology*, 79, 661-674

636 Sala, M., & Güde, H. (1999). Role of protozoans on the microbial ectoenzymatic  
637 activity during the degradation of macrophytes. *Aquatic Microbial Ecology*, 20, 75-82

638 Sala, M.M., Aparicio, F.L., Balagué, V., Boras, J.A., Borrull, E., Cardelús, C., Cros, L.,  
639 Gomes, A., López-Sanz, A., Malits, A., Martínez, R.A., Mestre, M., Movilla, J.,  
640 Sarmiento, H., Vázquez-Domínguez, E., Vaqué, D., Pinhassi, J., Calbet, A., Calvo, E.,  
641 Gasol, J.M., Pelejero, C., & Marrasé, C. (2016). Contrasting effects of ocean  
642 acidification on the microbial food web under different trophic conditions. *ICES*  
643 *Journal of Marine Science: Journal du Conseil*, 73, 670-679

644 Sala, M.M., Peters, F., Gasol, J.M., Pedrós-Alió, C., Marrasé, C., & Vaqué, D. (2002).  
645 Seasonal and spatial variations in the nutrient limitation of bacterioplankton growth in  
646 the northwestern Mediterranean. *Aquatic Microbial Ecology*, 27, 47-56

647 Scoullou, M., Plavšić, M., Karavoltzos, S., & Sakellari, A. (2006). Partitioning and  
648 distribution of dissolved copper, cadmium and organic matter in Mediterranean marine

649 coastal areas: The case of a mucilage event. *Estuarine, Coastal and Shelf Science*, 67,  
650 484-490

651 Smith, D.C., Simon, M., Alldredge, A.L., & Azam, F. (1992). Intense hydrolytic  
652 enzyme-activity on marine aggregates and implications for rapid particle dissolution  
653 *Nature*, 359, 139-142

654 Taylor, J.D., Cottingham, S.D., Billinge, J., & Cunliffe, M. (2014). Seasonal microbial  
655 community dynamics correlate with phytoplankton-derived polysaccharides in surface  
656 coastal waters. *ISME J*, 8, 245-248

657 Thingstad, T.F., Hagstrom, A., & Rassoulzadegan, F. (1997). Accumulation of  
658 degradable DOC in surface waters: Is it caused by a malfunctioning microbial loop?  
659 *Limnology and Oceanography*, 42, 398-404

660 Vicente, I., Ortega-Retuerta, E., Romera, O., Morales-Baquero, R., & Reche, I. (2009).  
661 Contribution of transparent exopolymer particles to carbon sinking flux in an  
662 oligotrophic reservoir. *Biogeochemistry*, 96, 13-23

663 Vila-Reixach, G., Gasol, J.M., Cardelus, C., & Vidal, M. (2012). Seasonal dynamics  
664 and net production of dissolved organic carbon in an oligotrophic coastal environment.  
665 *Marine Ecology-Progress Series*, 456, 7-19

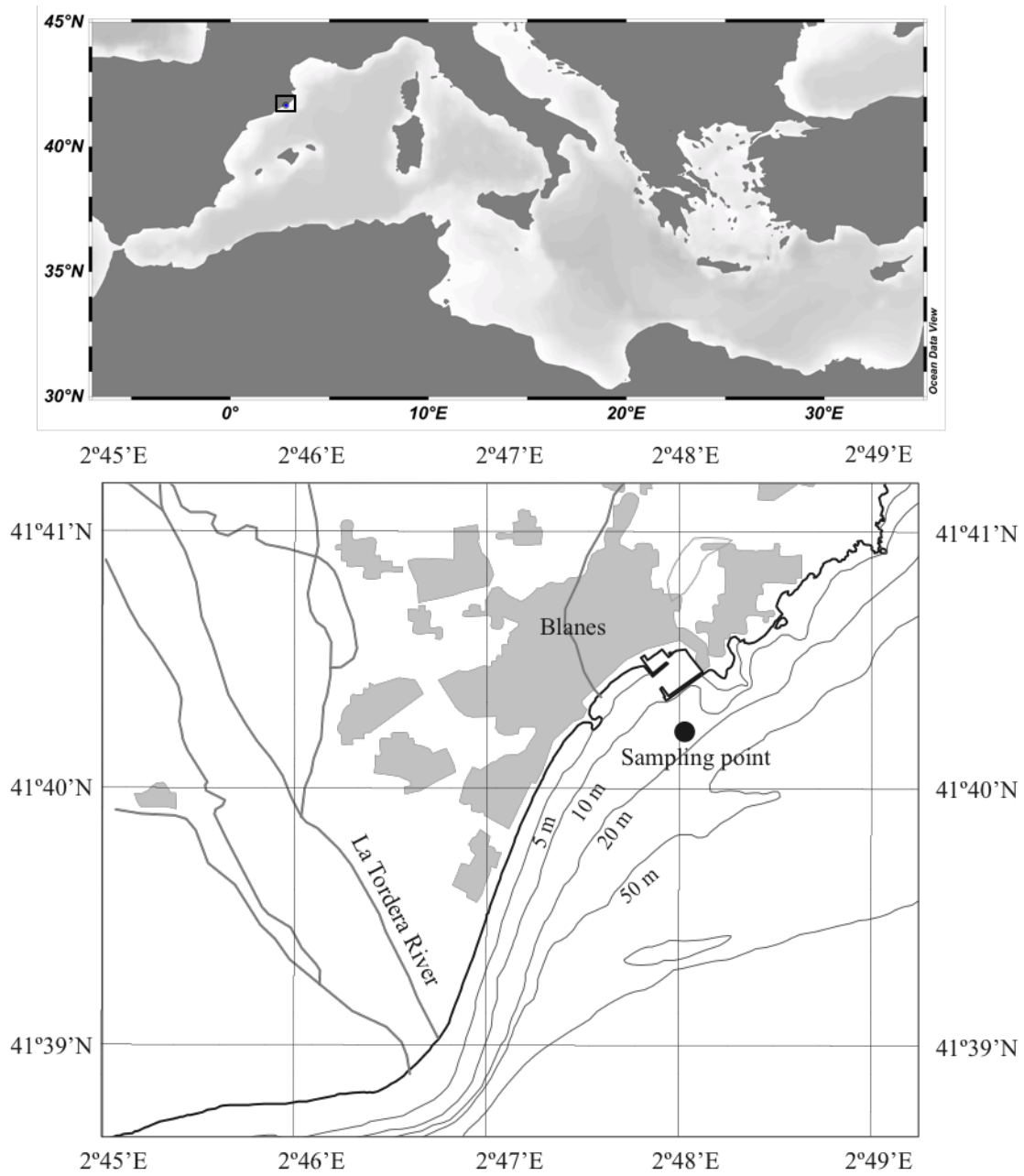
666 Wurl, O., Stolle, C., Van Thuoc, C., The Thu, P., & Mari, X. (2016). Biofilm-like  
667 properties of the sea surface and predicted effects on air-sea CO<sub>2</sub> exchange. *Progress*  
668 *in Oceanography*, 144, 15-24

669 Zhou, J., Mopper, K., & Passow, U. (1998). The role of surface-active carbohydrates in  
670 the formation of transparent exopolymer particles by bubble adsorption of seawater.  
671 *Limnology and Oceanography*, 43, 1860-1871

672

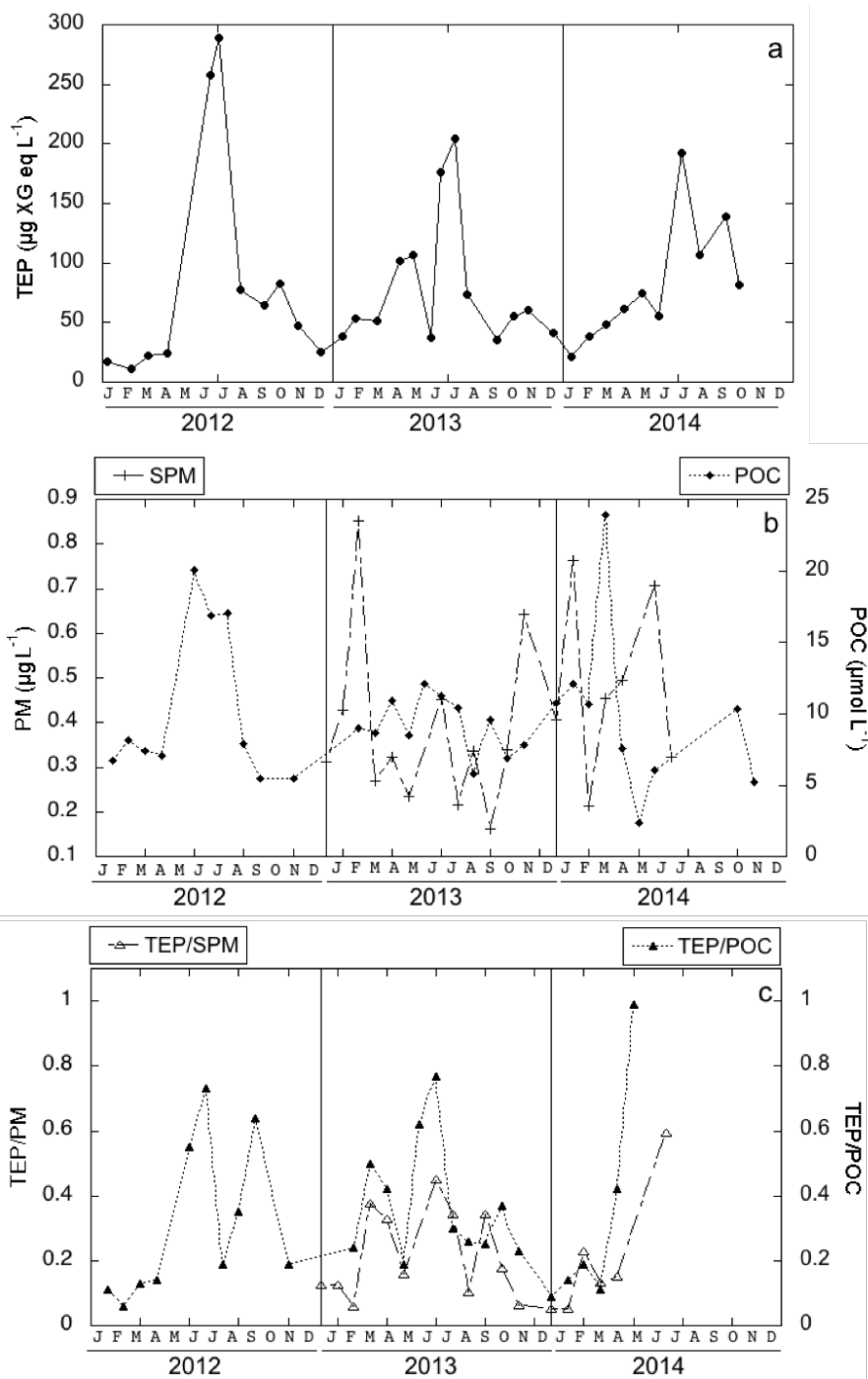
673

674 Figure 1. Map showing the study station.  
675  
676



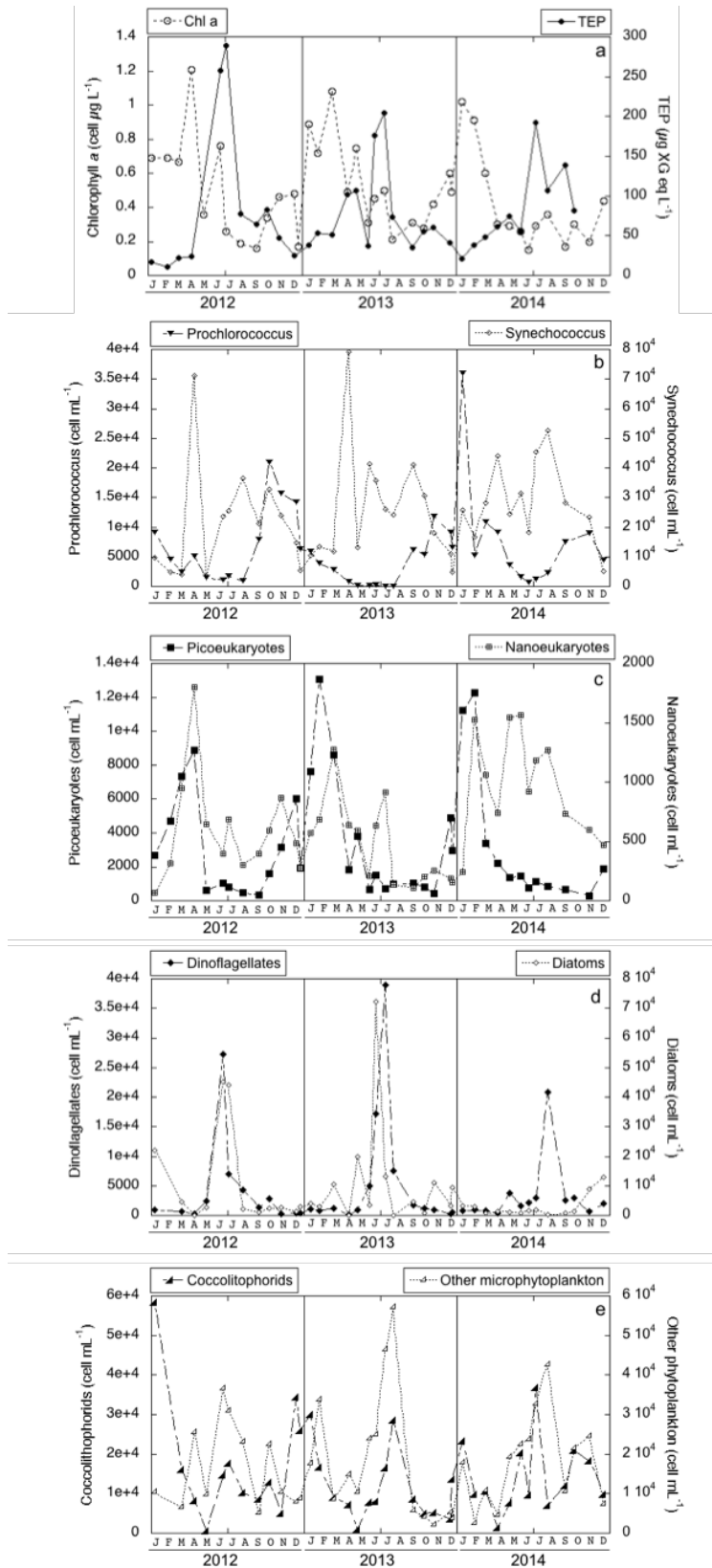
677

678 Fig. 2. Monthly average values of transparent exopolymer particles (TEP, a), particulate  
 679 matter (PM, b), and particulate organic carbon concentrations (POC, c) and TEP/PM  
 680 and TEP/POC (in g/g) ratios (d) over the three-year study



681  
 682

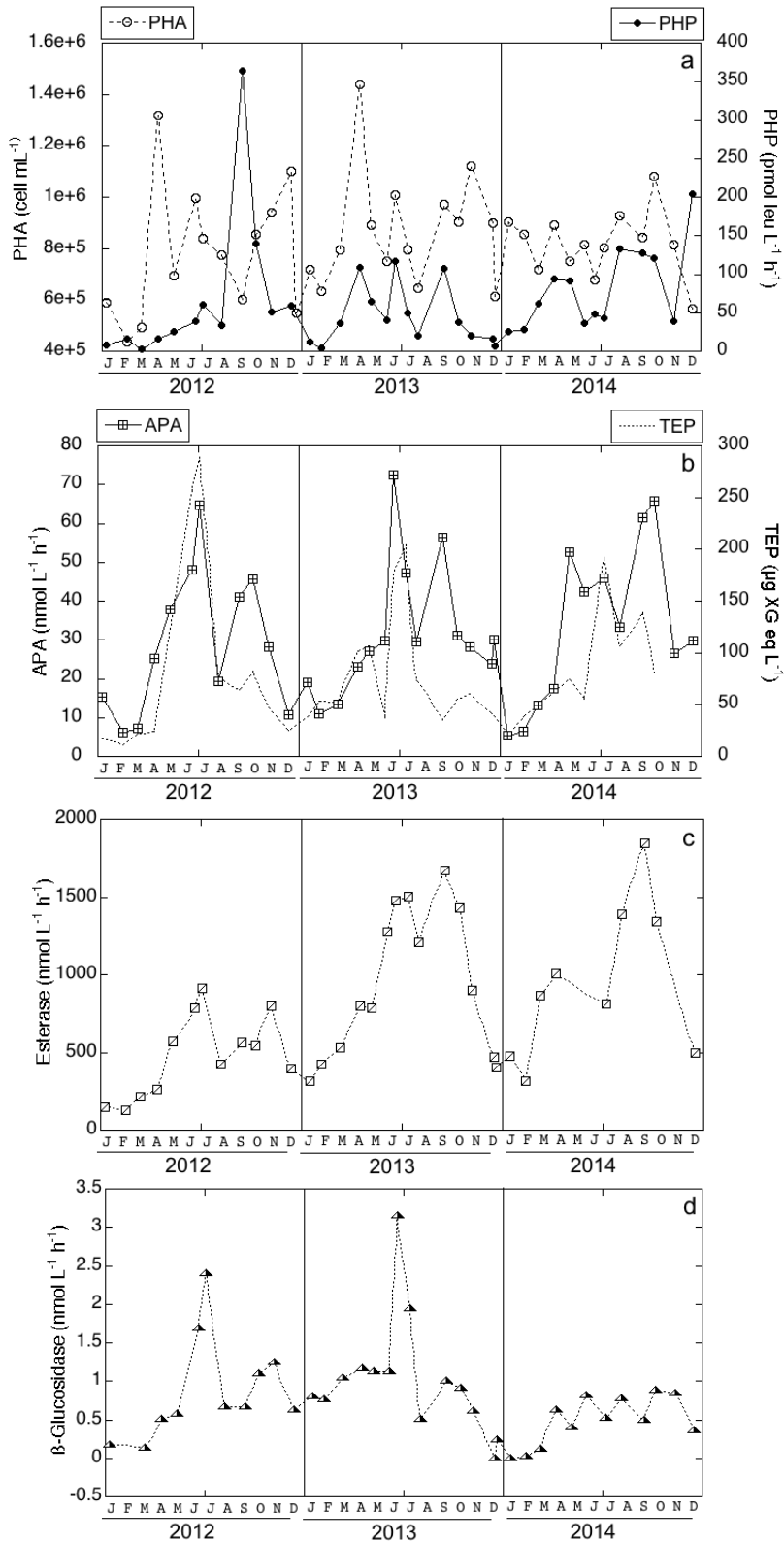
683 Fig 3. Dynamics of Chlorophyll *a* and TEP concentration (a); *Prochlorococcus* and  
 684 *Synechococcus* abundances (b); pico- and nanoeukaryote abundances (c); dinoflagellate  
 685 and diatom abundances (d); and coccolithophore and other microplankton groups  
 686 abundances (e) in Blanes Bay during the 2012-2014 period.



687  
 688

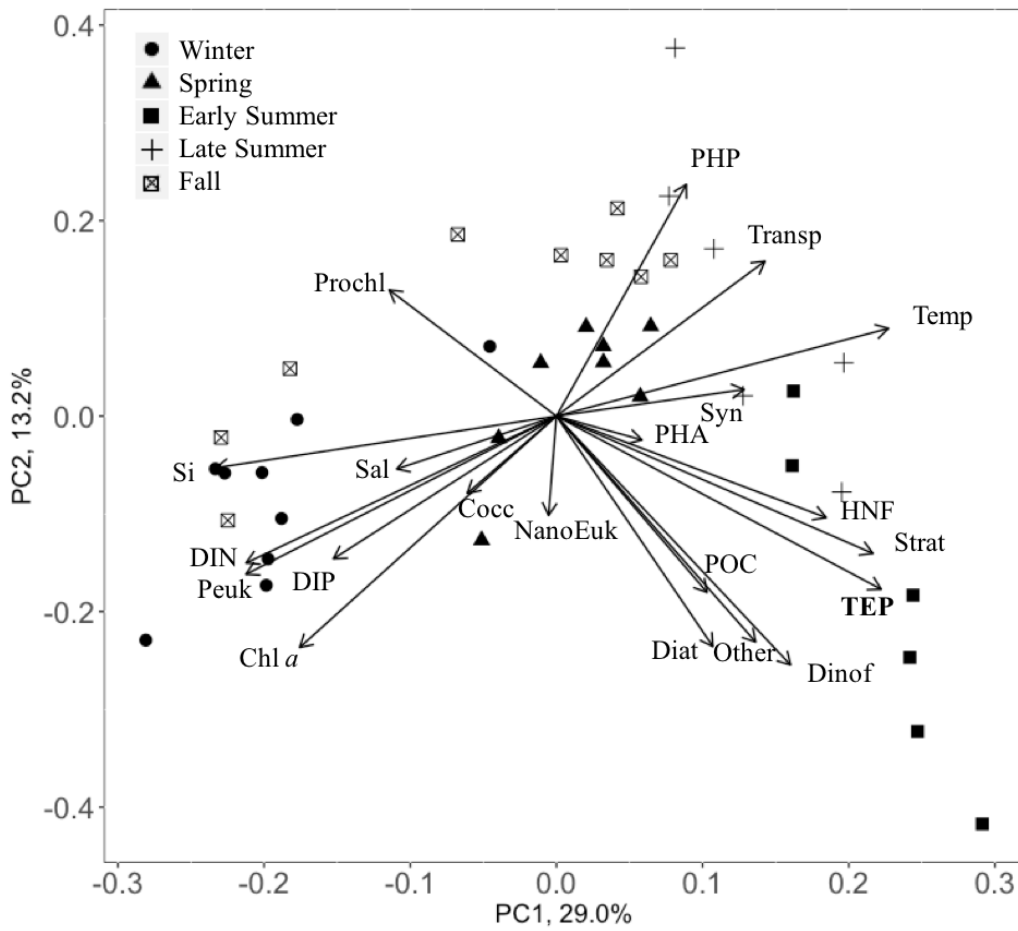
689 Fig. 4. Dynamics of prokaryotic heterotrophic abundance (PHA, a) and prokaryotic  
 690 heterotrophic activity (PHP, a); alkaline phosphatase activity (APA, b), esterase  
 691 activity (c); and  $\beta$ -glucosidase activity (d) in Blanes Bay during the 2012-2014 period.  
 692 TEP dynamics are presented in panel 4b to facilitate comparisons

693



694

695 Figure 5. Principal component analysis (PCA) of all samples from Blanes Bay. Each  
 696 Principal component (PC) is accompanied by its explained variation (%). The major  
 697 loading on PC1 include Temperature (Temp), transparent exopolymer particles (TEP)  
 698 and stratification index (Strat). The major loadings on PC2 include chlorophyll a (Chl  
 699 *a*), diatoms (diat), dinoflagellates (Dinof) and prokaryotic heterotrophic production  
 700 (PHP)  
 701  
 702



703  
 704

705 Table 1. Averages of the main physical and biological variables at each season  
 706 measured in the Blanes Bay time series between 2012 and 2014. Mann Whitney  
 707 pairwise tests with Bonferroni corrections are used to test for significant differences  
 708 among seasons. Significantly different groups ( $p < 0.05$ ) are labeled with different  
 709 letters (a, b, c). **DIN: Dissolved inorganic nitrogen. PP: Primary Production. POC:**  
 710 **Particulate organic carbon. TEP: Transparent exopolymer particles. PM: Particulate**  
 711 **Matter. PHA: Prokaryote heterotrophic abundance. PHP: Prokaryote heterotrophic**  
 712 **production. HNF: Heterotrophic nanoflagellates**

713

Variable	Winter Average ( $\pm$ SD)	Spring Average ( $\pm$ SD)	Summer Average ( $\pm$ SD)	Fall Average ( $\pm$ SD)
Temperature ( $^{\circ}$ C)	13.4 $\pm$ 0.7 a	15.6 $\pm$ 1.4 b	22.4 $\pm$ 1.7 c	17.7 $\pm$ 2.6 d
Salinity	38.15 $\pm$ 0.10 a	37.90 $\pm$ 0.22 a	37.99 $\pm$ 0.15 a	38.01 $\pm$ 0.12 a
Stratification Index ( $^{\circ}$ C)	0.05 $\pm$ 0.07 a	0.45 $\pm$ 0.34 b	2.80 $\pm$ 1.54 c	0.32 $\pm$ 0.95 ab
Water transparency (m)	14.0 $\pm$ 3.9 a	16.1 $\pm$ 2.7 a	17.3 $\pm$ 2.2 a	13.7 $\pm$ 4.3 a
DIN ( $\mu$ M)	2.39 $\pm$ 1.01 a	1.52 $\pm$ 0.69 ab	0.77 $\pm$ 0.46 b	1.61 $\pm$ 1.17 ab
PO <sub>4</sub> ( $\mu$ M)	0.11 $\pm$ 0.03 a	0.07 $\pm$ 0.03 a	0.08 $\pm$ 0.02 a	0.09 $\pm$ 0.06 a
<b>N/P</b>	<b>21.7 <math>\pm</math> 5.6 a</b>	<b>22.3 <math>\pm</math> 6.6 a</b>	<b>12.2 <math>\pm</math> 8.3 a</b>	<b>16.7 <math>\pm</math> 10.6 a</b>
SiO <sub>4</sub> ( $\mu$ M)	1.67 $\pm$ 0.67 a	1.19 $\pm$ 0.37 a	0.73 $\pm$ 0.21 b	1.27 $\pm$ 0.55 ab
Chl <i>a</i> ( $\mu$ g L <sup>-1</sup> )	0.72 $\pm$ 0.23 a	0.50 $\pm$ 0.33 a	0.32 $\pm$ 0.18 b	0.39 $\pm$ 0.12 b
PP ( $\mu$ g L <sup>-1</sup> h <sup>-1</sup> )	<b>0.45 <math>\pm</math> 0.05 a</b>	<b>1.16 <math>\pm</math> 0.11 a</b>	<b>0.86 <math>\pm</math> 0.55 a</b>	<b>0.58 <math>\pm</math> 0.36 a</b>
POC ( $\mu$ M)	9.2 $\pm$ 2.0 a	9.9 $\pm$ 6.7 a	11.9 $\pm$ 5.1 a	7.3 $\pm$ 2.1 a
TEP ( $\mu$ g XG eq L <sup>-1</sup> )	33.7 $\pm$ 15.9 a	65.9 $\pm$ 30.9 ab	147.0 $\pm$ 83.4 b	56.2 $\pm$ 20.9 ab
PM (mg L <sup>-1</sup> )	0.50 $\pm$ 0.25 a	0.36 $\pm$ 0.11 a	0.41 $\pm$ 0.19 a	0.38 $\pm$ 0.24 a
PHA ( $\times 10^5$ cell mL <sup>-1</sup> )	6.64 $\pm$ 1.49 a	9.45 $\pm$ 2.80 b	8.24 $\pm$ 1.37 b	9.21 $\pm$ 1.74 b
PHP (pmol leu L <sup>-1</sup> h <sup>-1</sup> )	20.8 $\pm$ 18.3 a	59.8 $\pm$ 35.2 ab	95.5 $\pm$ 93.5 b	76.6 $\pm$ 64.2 ab
HNF ( $\times 10^3$ cell mL <sup>-1</sup> )	0.59 $\pm$ 0.18 a	1.13 $\pm$ 0.64 ab	1.39 $\pm$ 0.55 b	0.76 $\pm$ 0.28 a
$\beta$ -Glucosidase (nmol L <sup>-1</sup> h <sup>-1</sup> )	0.37 $\pm$ 0.39 a	0.80 $\pm$ 0.31 a	1.26 $\pm$ 0.91 a	0.73 $\pm$ 0.38 a
Leucine-Aminopeptidase (nmol L <sup>-1</sup> h <sup>-1</sup> )	9.86 $\pm$ 11.92 a	30.35 $\pm$ 10.47 a	20.54 $\pm$ 17.08 a	13.17 $\pm$ 11.10 a
Alkaline Phosphatase (nmol L <sup>-1</sup> h <sup>-1</sup> )	12.71 $\pm$ 7.55 a	32.01 $\pm$ 11.57 b	47.27 $\pm$ 15.97 b	32.26 $\pm$ 15.46 b
Esterase (nmol L <sup>-1</sup> h <sup>-1</sup> )	383.9 $\pm$ 216.6 a	783.3 $\pm$ 348.0 ab	1146.5 $\pm$ 470.3 b	796.6 $\pm$ 402.4 ab

714

715

716 Table 2. Correlations between transparent exopolymer particle (TEP) concentration and  
 717 other environmental and biological variables during the 2012-2014 period in Blanes  
 718 Bay

719

Variable	r	p	n
TEP			
Temperature (°C)	0.64	< 0.001	34
Salinity	-0.44	0.013	34
Stratification Index (°C)	0.60	< 0.001	34
Water transparency (m)		ns	
DIN (µM)		ns	
PO <sub>4</sub> (µM)		ns	
SiO <sub>4</sub> (µM)	-0.55	< 0.001	34
Chl <i>a</i> (µg L <sup>-1</sup> )	-0.45	0.007	34
PP (µg L <sup>-1</sup> h <sup>-1</sup> )		ns	
Synechococcus (cell mL <sup>-1</sup> )		ns	
Prochlorococcus (cell mL <sup>-1</sup> )		ns	
Diatoms (cell mL <sup>-1</sup> )	0.63	< 0.001	33
Dinoflagellates (cell mL <sup>-1</sup> )	0.65	< 0.001	33
Coccolithophorids (cell mL <sup>-1</sup> )		ns	
Other microplankton (cell mL <sup>-1</sup> )		ns	
Nanoplankton (cell mL <sup>-1</sup> )		ns	
Picoplankton (cell mL <sup>-1</sup> )		ns	
POC (µM)		ns	
PM (mg L <sup>-1</sup> )		ns	
PHA (x10 <sup>5</sup> cell mL <sup>-1</sup> )		ns	
PHP (pmol leu L <sup>-1</sup> h <sup>-1</sup> )		ns	
HNF (x10 <sup>3</sup> cell mL <sup>-1</sup> )	0,59	< 0.001	34
β-Glucosidase (nmol L <sup>-1</sup> h <sup>-1</sup> )	0.69	< 0.001	33
Leucine-Aminopeptidase (nmol L <sup>-1</sup> h <sup>-1</sup> )		ns	
Alkaline Phosphatase (nmol L <sup>-1</sup> h <sup>-1</sup> )	0.66	< 0.001	34
Esterase (nmol L <sup>-1</sup> h <sup>-1</sup> )	0.60	< 0.001	32

720

721